Site-specific elevation of IL-1β and MMP-9 in the Willis circle by hemodynamic changes is associated with rupture in a novel rat cerebral aneurysm model

Takeshi Miyamoto, MD[1]; David K. Kung, MD[2]; Keiko T. Kitazato, BS[1];
Kenji Yagi, MD, PhD[1]; Kenji Shimada, MD, PhD[1]; Yoshiteru Tada, MD, PhD[1];
Masaaki Korai, MD[1]; Yoshitaka Kurashiki, MD[1]; Tomoya Kinouchi, MD, PhD[1];
Yasuhisa Kanematsu, MD, PhD[1]; Junichiro Satomi, MD, PhD[1];
Tomoki Hashimoto, MD[3]; Shinji Nagahiro, MD, PhD[1]

[1]Department of Neurosurgery, Institute of Biomedical Sciences, Tokushima University Graduate School, Tokushima, Japan

[2]Department of Neurosurgery, University of Pennsylvania, Philadelphia, USA

[3]Department of Anesthesia and Perioperative Care, University of California, San Francisco, USA

Correspondence to:

Takeshi Miyamoto, MD

Department of Neurosurgery

Institute of Biomedical Sciences

Tokushima University Graduate School

3-18-15 Kuramoto-cho, Tokushima 770-8503, Japan

TEL: 81-88-633-7149

FAX: 81-88-632-9464

E-mail: takeshi_edit@yahoo.co.jp

Sources of funding:

This work was supported by a Grant-in-Aid for Scientific Research [JSPS KAKENHI Grant Number JP15H04950], a Grant-in-Aid for Young Scientists (B) [JSPS KAKENHI Grant Number JP15K19972], and a Grant-in-Aid for the Strategic Young Researcher Overseas Visits Program for Accelerating Brain Circulation from the Japan Society for the Promotion of Science [JSPS KAKENHI Grant Number JPS2407].

Cover title: Rupture related to site-specific MMP-9 elevation

Word count of manuscript: 5038

Word count of abstract: 199

Abstract

The pathogenesis of subarachnoid hemorrhage (SAH) remains unclear. No models of cerebral aneurysms elicited solely by surgical procedures and diet have been established. Elsewhere we reported that only few rats in our original rat aneurysm model manifested rupture at the anterior- and posterior Willis circle (AW, PW) and that many harbored unruptured aneurysms at the anterior cerebral artery-olfactory artery bifurcation (ACA-OA). This suggests that rupture was site-specific. To test our hypothesis that a site-specific response to hemodynamic changes is associated with aneurysmal rupture, we modified our original aneurysm model by altering the hemodynamics. During 90-day observation, the incidence of ruptured aneurysms at the AW and PW was significantly increased and the high incidence of unruptured aneurysms at the ACA-OA persisted. This phenomenon was associated with an increase in the blood flow volume (BFVo). Notably, the level of matrix metalloproteinase (MMP)-9 associated with interleukin (IL)-1β was augmented by the increase in the BFVo, suggesting that these molecules exacerbated the vulnerability of the aneurysmal wall. The current study first demonstrates that a site-specific increase in IL-1β and MMP-9 elicited by hemodynamic changes is associated with rupture. Our novel rat model of rupture may help to develop pharmaceutical approaches to prevent rupture.

Key words: Animal Models, Cerebral Hemodynamics, Inflammation, Intracranial Aneurysm, Subarachnoid Hemorrhage

Introduction

Cerebral aneurysms are a major cause of subarachnoid hemorrhage (SAH). Despite the catastrophic consequences of aneurysmal rupture, not all mechanisms underlying the formation, progression, and rupture of cerebral aneurysms are fully understood.

In their rat aneurysm model, Hashimoto et al.[1] induced hemodynamic changes by right common carotid artery (CCA) ligation and renal hypertension by ligation of the bilateral posterior renal arteries. They fed their rats a saline and β-aminopropionitrile diet to elicit disruption of the vascular wall. As epidemiological studies have shown that the incidence of aneurysmal SAH is higher in post- than premenopausal women and in men,[2] we modified their model and created a cerebral aneurysm model in oophorectomized rats.[3] In these animals the incidence of aneurysms at the anterior cerebral artery-olfactory artery bifurcation (ACA-OA) is high.[4] Elsewhere we reported aspects of the pathogenesis of aneurysm formation. We documented that estrogen deficiency and hypertension augmented the elevation of oxidative stress, exacerbated endothelial damage induced by hemodynamic

changes alone, and resulted in an increase in vascular degradation molecules.[5, 6] Some drugs effectively reduced the incidence of cerebral aneurysm formation.[7-9] Despite their high number, no aneurysms at the ACA-OA, and only a few located at the AW and PW ruptured. Our recent study[10] showed that in our model rats exposed to hyperhomocysteinemia (HHcy), the increase in rupture of aneurysms at the anterior- and posterior Willis circle (AW, PW) was accompanied by an imbalance in matrix metalloproteinase (MMP)-9 and the tissue inhibitor of metalloproteinase (TIMP2) and by an increase in interleukin (IL)-6; both were abrogated by treating these rats with folic acid. These findings indicate that aneurysmal rupture is associated with vascular degradation due to an imbalance in MMP-9 and TIMP2. However, we have no direct evidence for the site-specificity of aneurysmal rupture and the mechanisms leading to rupture remain to be elucidated.

Although the most important risk factor for rupture in humans is thought to be the aneurysm size and site,[11-13] little is known about the site-specificity of rupture. Hemodynamic flow patterns in aneurysms and surrounding vessels play a role in aneurysmal rupture.[14] Carotid artery occlusion leads to significant hemodynamic changes in the cerebral circulation and the collaterals in the circle of Willis and to an increased demand on the collateral circulation. Furthermore, carotid artery occlusion due to atherosclerosis,

iatrogenic ligation, or agenesis of the internal carotid artery (ICA) resulted in cerebral aneurysm formation.[15-17] While hemodynamic changes may be implicated in the formation and rupture of aneurysms, there is no direct evidence for their role in such events.

Based on these findings we modified our rat aneurysm model and tested the hypothesis that a site-specific response to hemodynamic changes elicits an imbalance in MMP-9 and TIMP2 and an increase in pro-inflammatory cytokines, thereby leading to vascular degradation and aneurysmal rupture.

Here we show that rats in our modified model manifest a high incidence of ruptured aneurysms under experimentally induced pathophysiological conditions and that their rupture in estrogen-deficient hypertensive rats is associated with a site-specific increase in the level of IL-1β and vascular degradation molecules induced by hemodynamic changes in the Willis circle.

Materials and Methods

All experiments and protocols were approved by the ethics committee of the Institute of Biomedical Sciences, Tokushima University Graduate School and conducted in accordance with the National Institutes of Health (NIH) Guide for the Care and Use of

Laboratory Animals. Experiments were reported according to the ARRIVE guidelines. Before any procedures the rats were anesthetized by 2-4% isoflurane inhalation.

Female Sprague-Dawley rats purchased from Charles River Laboratories Japan Inc. (Yokohama, Japan) were housed in a temperature- and humidity-controlled room (about 23^{o}C and 50%, respectively) under a 12-hr light cycle and allowed free access to food and water.

Aneurysm induction

Ten-week-old female rats (230-260 g, n=64) were divided into 2 equal groups. All rats were anesthetized by inhaling 2-4% isoflurane and by a subcutaneous injection of 0.25% bupivacaine. Group 1 underwent ligation of the left CCA; in group 2 we additionally ligated the right pterygopalatine- and the right external carotid artery (PPA, ECA) (Supplemental Fig. 1A). Immediately after left CCA ligation we performed oophorectomy. Subsequently the rats received a high salt diet (8% sodium chloride). Two weeks later, an investigator blinded to their group membership performed bilateral posterior renal artery ligation (RAL) to induce hypertension. The cause of death within 30 days was unclear in 5 group 1- and 6 group 2 rats; they were excluded from this study. Survivors exhibiting abnormal behavior or a drastic weight loss were euthanized by 4% isoflurane inhalation.

Those, and rats that died, were used by two blinded observers to assess aneurysmal rupture 30-90 days after the last procedure. Ruptured aneurysms were inspected under a stereomicroscope after removing the blood coagulum. We identified saccular aneurysms at the AW and PW that were 1.5 times larger than the parent artery. They were categorized as AW aneurysms when they had arisen at the anterior communicating artery (AcomA), the ACA, the ICA, or the right middle cerebral artery (MCA) and as PW aneurysms when they were located at the proximal portion of the left posterior cerebral artery (P1). As shown in Figure 1A, we prepared vascular corrosion casts 90 days after RAL and examined the unruptured aneurysms.[18] The right ACA-OA and the Willis circle on the casts were inspected under a scanning electron microscope (SEM, VE8800, Keyence, Osaka, Japan). Based on morphological findings the vascular wall surface was recorded as harboring a cerebral aneurysm when there was moderate outward evagination or an obvious saccular formation at the ACA-OA bifurcation.

Transcranial duplex ultrasonography

The bilateral ICA (n=7 per group) and the basilar artery (BA, n=4 per group) were examined 4 weeks after RAL by simple random sampling without replacement.

Cell culture

We used human brain vascular smooth muscle cells (HBVSMCs; ScienCell Research Laboratories, Carlsbad, CA, USA) from passages 5 to 8. They were grown in smooth muscle cell medium (ScienCell) in 10-mm polystyrene plates. After 24-hr treatment with recombinant human IL-1β (Wako, Osaka, Japan) (1 ng/ml), the cells were harvested for quantitative real-time polymerase chain reaction (qRT-PCR) assay. Cell proliferation was determined with the Cell Counting Kit-8 (Dojindo Laboratories, Kumamoto, Japan) in 24-well plates.

RNA isolation and qRT-PCR assay

Samples from another set of sham-operated-, group 1- and group 2 rats (n=8 each) were subjected to qRT-PCR assay. Five weeks after RAL these rats were euthanized and total RNA from the right ACA-OA, the right P1 and the left P1 was isolated and extracted. At the time of sampling no aneurysms had ruptured. We examined the level of MMP-9, TIMP2, IL-1β, IL-6, tumor necrosis factor (TNF)-α, and glyceraldehyde 3-phosphate dehydrogenase (GAPDH). The results were normalized to GAPDH.

Statistical analysis

Power estimates were calculated based on $\alpha = 0.05$, $1\text{-}\beta = 0.8$, and a surgery-related drop-out rate of 10-20% to obtain group sizes appropriate for detecting an effect size of 0.4 *in vivo* based on a preliminary experiment using G*Power 3.1. The highest failures were death after bilateral RAL. The survival rate was analyzed with the log-rank test, the incidence of aneurysms with the Fisher exact test, and sequentially obtained data with analysis of variance (ANOVA) followed by the Tukey-Kramer test for multiple comparisons. The mRNA expression levels were determined with Kruskal-Wallis test followed by the Wilcoxon signed-rank test with Bonferroni correction for comparing samples from the same individuals and the Mann-Whitney *U*-test with Bonferroni correction for three-group comparisons. We calculated the Spearman rank correlation (r) to characterize the correlation strength between IL-1β and MMP-9. Statistical analyses were performed using IBM SPSS Statistics 22. Data are shown as the mean ± SD. Differences were considered statistically significant at $p < 0.05$.

Results

Additive hemodynamic changes increased the incidence of ruptured AW and PW aneurysms without affecting the blood pressure and the incidence of ACA-OA aneurysms

In our model rats with aneurysms induced under pathophysiological conditions elicited by surgical procedures and diet alone, we detected SAH from the rupture of AW and PW aneurysms (Fig. 1B); no aneurysms at the ACA-OA ruptured. We euthanized rats manifesting a 10% loss in body weight, hemiparesis, or chronic convulsions during the observation period and looked for ruptured aneurysms. Vascular casts[18] were prepared on day 90 to examine unruptured AW-, PW-, and ACA-OA aneurysms.

In the course of 90 days, the incidence of SAH was significantly higher in group 2- than group 1 rats with ruptured aneurysms ($p < 0.01$, Fig. 1C). Significantly more group 2- than group 1 rats suffered aneurysmal rupture (50% vs 11%, $p < 0.01$, Fig. 1D). The total incidence of ruptured- and unruptured aneurysms was also significantly higher in group 2 (58% vs 22%, $p < 0.01$), suggesting that hemodynamic changes were involved. The rupture rate (the number of ruptured aneurysms/total number of aneurysms at the AW and PW) was high in group 2 (81%) and group 1 rats (50%), indicating that AW and PW aneurysms were unstable and prone to rupture in both groups. As shown in Figure 2A, on corrosion casts, unruptured aneurysms were remarkably larger at the AW and PW than at the ACA-OA. The

incidence of ACA-OA aneurysms was similar in both groups and high (around 80%). However, ACA-OA aneurysms did not rupture, indicating that they were stable (Fig. 2B). These findings point to site-specificity of aneurysmal growth and rupture.

Throughout the observation period, until rupture onset, the blood pressure (Supplemental Fig. IB) and body weight (data not shown) of the experimental rats did not change significantly.

Histopathologically, the ruptured rat PW aneurysms resembled human saccular cerebral aneurysms

The wall of ruptured saccular cerebral aneurysms in humans is characterized by a disruption of the internal elastic lamina in the intima and a decellularized, degenerated matrix in the media.[19] We histopathologically assessed the ruptured PW aneurysm from a euthanized group 2 rat that exhibited drastic weight loss 40 days after RAL. We observed a poorly organized luminal thrombus in the lumen, disruption of the internal elastic lamina in the intima, loss of mural cells, a degenerated matrix, and hyalinization in the thickened media of the ruptured PW aneurysm (Fig. 3). The features of the rat ruptured PW aneurysms resembled those seen in the wall of human ruptured saccular cerebral aneurysms.

The higher incidence of ruptured PW aneurysms in group 2 rats was associated with an increase in the blood flow volume (BFVo) in the BA

To confirm the presence of hemodynamic changes, we obtained ultrasonograms in group 1 and 2 rats that had undergone carotid artery ligation 6 weeks earlier. The antegrade peak systolic velocity (PSV) and the end-diastolic velocity (EDV) in the right ICA and the BA were significantly higher and the retrograde PSV in the left ICA was lower in both experimental groups than in sham-operated rats (Figs. 4A, 4B). Therefore, ultrasonography confirmed hemodynamic changes (Fig. 4D). The rise in the mean flow velocity (MFV) in the right ICA and the BA of both groups was significantly higher than in the shams (Fig. 4C). It was somewhat higher in group 2 than group 1; the difference was not statistically significant.

As shown in Figure 5A, the diameter of the right ICA and the left P1 was increased in both experimental groups. Notably, the diameter of the BA was larger in group 2 than in group 1. The BFVo[20] was calculated from the MFV and the vascular diameter using the equations:

$$MFV\ (v) = (PSV\text{-}EDV)/3 + EDV$$

$$BFVo = 1/4\ \pi r^2 v\ (r = \text{the vessel diameter}).$$

The BFVo was significantly larger in the right ICA and BA of both experimental groups than in sham rats. As the diameter of- and the MFV in the right ICA and BA were somewhat greater in group 2 than in group 1, the BFVo in the BA was significantly greater in group 2 ($p < 0.05$, Fig. 5B) and the BFVo in the right ICA was a little greater in group 2 than group 1 although the difference was not statistically significant. The incidence of ruptured AW and PW aneurysms was 2-3 times higher in group 2 than group 1 (Fig. 5C). These observations show that in both experimental groups the BFVo in the right ICA and BA was increased and that additive ligation of the right PPA and ECA increased the BFVo in the BA. Although we could not directly assess the BFVo in the AcomA, the left P1, and other arteries in the Willis circle, we think that the increased incidence of ruptured AW and PW aneurysms may be associated with the increased BFVo in the right ICA and BA, respectively. Despite the higher incidence of rupture of AW and PW aneurysms, the incidence of unruptured ACA-OA aneurysms was not affected by hemodynamic changes. These observations confirm the site-specific vulnerability of vessels in the Willis circle exposed to hemodynamic changes.

The mRNA level of MMP-9 was higher in the vascular wall of the left P1 in group 2- than group 1 rats

To identify molecules related to the difference in the vulnerability to rupture of aneurysms in group 2 rats we compared the mRNA level of inflammation-related and vascular degradation molecules at the left P1 of sham-, group 1-, and group 2 rats. As shown in Figure 6A, in both experimental groups the mRNA level of IL-1β and MMP-9 was significantly higher than in the shams (Fig. 6A). Furthermore, the mRNA level of MMP-9 was higher in group 2- than group 1 rats. These findings suggest that the expression of IL-1β and MMP-9 was induced in group 1- and 2 rats and that additive carotid ligation resulted in a greater increase in MMP-9 in group 2 rats.

MMP-9 expression was higher in the vascular wall of the left P1 than in other arteries of group 2 rats

To further address the site-specific vulnerability in the Willis circle, we compared the mRNA level of IL-1β, MMP-9, and TIMP2 at the right and left P1, and the ACA-OA of group 2 rats. As shown in Figure 6B, the mRNA level of IL-1β was significantly higher at the ACA-OA and the left P1 than at the right P1 ($p < 0.01$). The mRNA level of MMP-9 was highest at the left P1 and positively correlated with the mRNA level of IL-1β ($r = 0.46$, $p < 0.05$). Furthermore, there was an evident imbalance between MMP-9 and TIMP2 at the left P1. These findings suggest that the site-specific overwhelming expression of

degradation molecules induced by hemodynamic changes in the Willis circle increased the propensity of PW aneurysms to rupture.

IL-1β upregulated the expression of MMP-9 and increased cell proliferation in human brain vascular smooth muscle cells (HBVSMCs) *in vitro*

MMP-9 activity is increased by IL-1β in cardiac fibroblasts *in vitro*.[21] To confirm the effect of IL-1β on MMP-9, we used HBVSMCs. We found that the mRNA level of MMP-9 but not of TIMP2 was increased and that the proliferation of HBVSMCs exposed to IL-1β was increased (Fig. 7).

Discussion

We first document the high, reproducible incidence of ruptured aneurysms at the AW, PW and of unruptured aneurysms at the ACA-OA in rats exposed to hemodynamic changes under pathophysiological conditions elicited by surgical procedures and diet alone. We addressed the site-specific characteristics of these aneurysms and found that AW and PW aneurysms did, while ACA-OA aneurysms did not rupture. We show that rupture was

at least partly associated with a site-specific elevation of IL-1β and an imbalance in MMP-9 and TIMP2 induced by hemodynamic changes.

Our earlier study[3] found that estrogen-deficient hypertensive female rats subjected to ligation of the left CCA had a high incidence of aneurysms at the ACA-OA bifurcation. While none of those aneurysms ruptured, some aneurysms at the AW and PW ruptured. To induce a higher rupture rate, in the current study we ligated, in addition to the left CCA, the right ECA and the right PPA (group 2). As expected, the additive hemodynamic changes elicited in those rats resulted in a higher incidence in the formation and rupture of aneurysms at the AW and PW. Histopathologically, the ruptured PW aneurysms resembled saccular cerebral aneurysms in humans. Cai et al.[22] reported that while hemodynamic changes after the ligation of the unilateral CCA, contralateral PPA, and the ECA induced aneurysms in normotensive male rats, their incidence was low. In an earlier study[3, 23] we induced cerebral aneurysms in male and female rats. We found that while few males developed aneurysms, in oophorectomized rats we encountered a high incidence of cerebral aneurysms. Those findings suggested the protective role of estrogen against vascular damage. Besides the vascular degeneration elicited by exposing the current rats to estrogen deficiency, renal hypertension, and a high salt diet, the additive hemodynamic changes we induced may have contributed to the high incidence of aneurysmal rupture.

To assess the hemodynamic changes elicited by additive carotid artery ligation, we first recorded blood flow velocity (BFVe) changes observed on ultrasonograms, which are thought to be useful for evaluating the intracranial cerebral blood flow in rats.[24] We detected an increase in the BFVe in the cerebral arteries of our experimental rats. Then we used SEM to study the aneurysms and to determine the vascular diameter on corrosion casts. We observed the outward remodeling of the ICA and the left P1 in these rats. We suspect that the higher incidence of ruptured PW aneurysms in group 2- than group 1 rats was associated with the increased BFVo in the BA. Earlier studies in rabbits[25, 26] suggested that an increase in the blood flow results in adaptive vascular remodeling and the formation of aneurysms. Quantitative computational hemodynamic analysis showed that aneurysmal growth is associated with an increased risk for rupture.[27, 28] These findings support our hypothesis that hemodynamic changes are associated with aneurysmal growth and rupture. To further address the effects of altered hemodynamics, we compared the mRNA level of IL-1β, MMP-9, and its inhibitor, TIMP2, in the left P1 of our experimental and sham rats. We found that the increase in MMP-9 was associated with a higher incidence of PW aneurysms in group 2.

Despite the high incidence (around 80%) of ACA-OA aneurysms in both experimental groups there was no increase in their rupture. This suggests a site-specific

response to hemodynamic changes and a difference in the pathogenesis underlying the formation and rupture of cerebral aneurysms. To better understand the vulnerability of the left P1 in group 2 rats that manifested a high incidence of aneurysmal rupture we assessed inflammatory-related and vascular degradation molecules and compared their levels at the vulnerable left P1 with seemingly less vulnerable sites, the ACA-OA bifurcation and the right P1. TNF-α is thought to play a highly important role in vascular inflammation which, in turn, has a pivotal role in aneurysmal progression.[9, 29-32] Hemodynamic stress and induced hypertension increased the expression of TNF-α in rats[29] while the TNF-α inhibitors etanercept and 3,6´dithiothalidomide (DTH) decreased the rate of aneurysm formation and rupture.[31, 32] As we observed no difference in the mRNA level of TNF-α and IL-6 at the left P1 and other arteries in group 2 rats (data not shown), we think that it does not contribute to aneurysmal rupture.

There was a significant increase in MMP-9, a decrease in TIMP2, and an imbalance in these molecules at the left P1 of group 2 rats. In agreement with the current study, elsewhere[10] we reported that in our oophorectomized aneurysm model rats treated with HHcy, AW and PW aneurysms were prone to rupture and we documented the disequilibrium in MMP-9 and TIMP2 and the increased infiltration of macrophages at the AW. Associated with the increase in MMP-9, the expression of IL-1β was increased at the

left P1; this phenomenon was observed in neither our sham rats nor in the right P1 of experimental rats where no aneurysms were detected. IL-1β, one of the key inflammatory mediators in cerebrovascular inflammation,[33] cerebral aneurysms,[34] and aortic aneurysms, promotes extracellular matrix degradation by increasing the production of MMPs.[35] Zhang et al.[36] demonstrated that in humans, activation of the nod-like receptor (NLR) family, the pyrin-domain containing 3 (NLRP3) and the NLRP3 inflammasome-mediated production of mature IL-1β, is associated with the rupture of cerebral aneurysms. We found that *in vitro* treatment of HBVSMCs with IL-1β increased their expression of MMP-9 and their proliferation. This was consistent with histological findings of a thickened media and a disrupted matrix. These findings partly support our hypothesis that an increase in MMP-9 and IL-1β elicited a disruption of the aneurysmal wall and the rupture of aneurysms. Further studies are needed to confirm the causal relationship between these molecules and aneurysmal rupture.

Inflammatory changes due to estrogen deficiency, hypertension, and altered hemodynamics may render the vascular wall at the AW and PW vulnerable. Based on current and earlier findings, we posit that in our model rats, increased levels of IL-1β in the vascular wall affected the degradation molecule MMP-9 and rendered the vulnerable aneurysmal wall prone to rupture (Fig. 7C). At present we cannot explain why there is a

site-specific increase in the level of IL-β and MMP-9 at the left P1. Studies are underway to determine whether the rate of aneurysmal rupture can be decreased by inhibiting the level of these molecules in group 2 rats.

In humans, carotid artery occlusion leads to significant hemodynamic changes in the cerebral circulation with collaterals in the circle of Willis and to the formation of intracranial aneurysms.[15-17] The most important risk factor for rupture is thought to be the aneurysm size and site.[11-13] The rupture of aneurysms we induced in our rats by eliciting hemodynamic changes was site-specific, therefore, their aneurysms may partly reflect the characteristics of human *de novo* aneurysms. Consequently, our modified rat aneurysm model may be useful for studying the formation, growth, and rupture of cerebral aneurysms in humans.

In summary, we provide new evidence that aneurysmal rupture in rats was partly attributable to a site-specific increase in MMP-9 associated with an increase in IL-1β induced by altered hemodynamics. Importantly, under the pathophysiological conditions we imposed, we observed aneurysmal rupture at sites in the circle of Willis of rats that are similar to those in humans. Furthermore, histopathologically, the ruptured rat aneurysms resembled human saccular cerebral aneurysms. Our group 2 rats may represent a good model for assessing the efficacy of pharmacological treatments to prevent aneurysmal

rupture. Currently we have no direct evidence for an association between aneurysms and pro-inflammatory- and degradation molecules and studies are underway to identify other pathophysiological factors that contribute to the rupture of aneurysms.

Acknowledgement

We thank Yoshiro Kanasaki, a medical student at Tokushima University, for his assistance and Yoshihiro Okayama, a biostatistician, for his assistance with the statistical analysis.

Sources of funding

This work was supported by a Grant-in-Aid for Scientific Research [JSPS KAKENHI Grant Number JP15H04950], a Grant-in-Aid for Young Scientists (B) [JSPS KAKENHI Grant Number JP15K19972], and a Grant-in-Aid for the Strategic Young Researcher Overseas Visits Program for Accelerating Brain Circulation from the Japan Society for the Promotion of Science [JSPS Grant Number JPS2407].

Authors' Contributions

TM, DKK, and KTK took part in the conception, design, acquisition of data, and the drafting of the article. MK and Yoshitaka Kurashiki participated in the acquisition and the analysis or interpretation of data. KY, KS, YT, TK, Yasuhisa Kanematsu, JS, TH, and SN critically reviewed the paper for intellectual content and approved its submission.

Declaration of conflicting interests

The authors declare no potential conflicts of interest with respect to the research, authorship, and/or publication of this article.

Supplementary material for this paper is available at:
http://jcbfm.sagepub.com/content/by/supplemental-data

References

1. Hashimoto N, Handa H, Hazama F. Experimentally induced cerebral aneurysms in rats. *Surg Neurol.* 1978; 10: 3-8
2. Harrod CG, Batjer HH, Bendok BR. Deficiencies in estrogen-mediated regulation of cerebrovascular homeostasis may contribute to an increased risk of cerebral aneurysm pathogenesis and rupture in menopausal and postmenopausal women. *Med Hypotheses*. 2006; 66: 736–756.
3. Jamous MA, Nagahiro S, Kitazato KT, et al. Role of estrogen deficiency in the formation and progression of cerebral aneurysms. Part I: Experimental study of the effect of oophorectomy in rats. *J Neurosurg*. 2005; 103: 1046-1051
4. Matsushita N, Kitazato KT, Tada Y, et al. Increase in body Na^+/water ratio is associated with cerebral aneurysm formation in oophorectomized rats. *Hypertension*. 2012; 60: 1309-1315
5. Tamura T, Jamous MA, Kitazato KT, et al. Endothelial damage due to impaired nitric oxide bioavailability triggers cerebral aneurysm formation in female rats. *J Hypertens.* 2009; 27: 1284-1292
6. Tada Y, Yagi K, Kitazato KT, et al. Reduction of endothelial tight junction proteins is related to cerebral aneurysm formation in rats. *J Hypertens*. 2010; 28: 1883-1891

7. Tada Y, Kitazato KT, Yagi K, et al. Statins promote the growth of experimentally induced cerebral aneurysms in estrogen-deficient rats. *Stroke*. 2011; 42: 2286-2293

8. Tada Y, Kitazato KT, Tamura T, et al. Role of mineralocorticoid receptor on experimental cerebral aneurysms in rats. *Hypertension*. 2009; 54: 552-557

9. Yagi K, Tada Y, Kitazato KT, et al. Ibudilast inhibits cerebral aneurysms by down-regulating inflammation-related molecules in the vascular wall of rats. *Neurosurgery*. 2010; 66: 551-555

10. Korai M, Kitazato KT, Tada Y, et al. Hyperhomocysteinemia induced by excessive methionine intake promotes rupture of cerebral aneurysms in ovariectomized rats. *J Neuroinflamm*. 2016; 13: 165

11. Morita A, Kirino T, Hashi K, et al. The natural course of unruptured cerebral aneurysms in a Japanese cohort. *New Engl J Med.* 2012; 366: 2474-2482

12. Sonobe M, Yamazaki T, Yonekura M, et al. Small unruptured intracranial aneurysm verification study: SUAVE study, Japan. *Stroke*. 2010; 41: 1969-1977

13. Wiebers DO, Whisnant JP, Huston J, 3rd, et al. Unruptured intracranial aneurysms: Natural history, clinical outcome, and risks of surgical and endovascular treatment. *Lancet*. 2003; 362: 103-110

14. Meng H, Tutino VM, Xiang J, et al. High WSS or low WSS? Complex interactions of hemodynamics with intracranial aneurysm initiation, growth, and rupture: Toward a unifying hypothesis. *Am J Neuroradiol*. 2014; 35: 1254-1262

15. Fujiwara S, Fujii K, Fukui M. *De novo* aneurysm formation and aneurysm growth following therapeutic carotid occlusion for intracranial internal carotid artery aneurysms. *Acta Neurochir.* 1993; 120: 20-25

16. Jamous MA, Abdel-Aziz H, Kaisy F. Collateral blood flow patterns in patients with unilateral ICA agenesis and cerebral aneurysm. *Neuroendocrinol Lett.* 2007; 28: 647-651

17. Arnaout OM, Rahme RJ, Aoun SG, et al. *De novo* large fusiform posterior circulation intracranial aneurysm presenting with subarachnoid hemorrhage 7 years after therapeutic internal carotid artery occlusion: Case report and review of the literature. *Neurosurgery*. 2012; 71: E764-771

18. Jamous MA, Nagahiro S, Kitazato KT, et al. Vascular corrosion casts mirroring early morphological changes that lead to the formation of saccular cerebral aneurysm: An experimental study in rats. *J Neurosurg*. 2005; 102: 532-535

19. Frösen J, Tulamo R, Paetau A, et al. Saccular intracranial aneurysms: Pathology and mechanisms. *Acta Neuropathol.* 2012; 123: 773-786

20. Kreis D, Schulz D, Stein M, et al. Assessment of parameters influencing the blood flow velocities in cerebral arteries of the rat using ultrasonographic examination. *Neurol Res*. 2011; 33: 389-395

21. Siwik DA, Chang DL, Colucci WS. Interleukin-1β and tumor necrosis factor-α decrease collagen synthesis and increase matrix metalloproteinase activity in cardiac fibroblasts *in vitro*. *Circ Res.* 2000; 86: 1259-1265

22. Cai J, He C, Yuan F, et al. A novel haemodynamic cerebral aneurysm model of rats with normal blood pressure. *J Clin Neurosci.* 2012; 19: 135-138

23. Jamous MA, Nagahiro S, Kitazato KT, et al. Vascular corrosion casts mirroring early morphological changes that lead to the formation of saccular cerebral aneurysm: An experimental study in rats. *J Neurosurg*. 2005; 102: 532-535.

24. Bonnin P, Debbabi H, Mariani J, et al. Ultrasonic assessment of cerebral blood flow changes during ischemia-reperfusion in 7-day-old rats. *Ultrasound Med Biol.* 2008; 34: 913-922

25. Hoi Y, Gao L, Tremmel M, et al. *In vivo* assessment of rapid cerebrovascular morphological adaptation following acute blood flow increase. *J Neurosurg.* 2008; 109: 1141-1147

26. Tutino VM, Mandelbaum M, Choi H, et al. Aneurysmal remodeling in the circle of Willis after carotid occlusion in an experimental model. *J Cereb Blood Flow Metab.* 2014; 34: 415-424

27. Xiang J, Natarajan SK, Tremmel M, et al. Hemodynamic-morphologic discriminants for intracranial aneurysm rupture. *Stroke*. 2011; 42: 144-152

28. Schneiders JJ, Marquering HA, van den Berg R, et al. Rupture-associated changes of cerebral aneurysm geometry: High-resolution 3D imaging before and after rupture. *Am J Neuroradiol.* 2014; 35: 1358-1362

29. Ali MS, Starke RM, Jabbour PM, et al. TNF-alpha induces phenotypic modulation in cerebral vascular smooth muscle cells: Implications for cerebral aneurysm pathology. *J Cerebr Blood Flow Metab.* 2013; 33: 1564-1573

30. Jayaraman T, Paget A, Shin YS, et al. TNF-alpha-mediated inflammation in cerebral aneurysms: A potential link to growth and rupture. *Vascular Health Risk Manage.* 2008; 4: 805-817

31. Starke RM, Chalouhi N, Jabbour PM, et al. Critical role of TNF-alpha in cerebral aneurysm formation and progression to rupture. *J Neuroinflamm*. 2014; 11: 77

32. Yokoi T, Isono T, Saitoh M, et al. Suppression of cerebral aneurysm formation in rats by a tumor necrosis factor-alpha inhibitor. *J Neurosurg*. 2014; 120: 1193-1200

33. Denes A, Drake C, Stordy J, et al. Interleukin-1 mediates neuroinflammatory changes associated with diet-induced atherosclerosis. *J Am Heart Assoc*. 2012; 1: e002006

34. Chalouhi N, Ali MS, Jabbour PM, et al. Biology of intracranial aneurysms: Role of inflammation. *J Cereb Blood Flow Metab*. 2012; 32: 1659-1676

35. Johnston WF, Salmon M, Pope NH, et al. Inhibition of interleukin-1β decreases aneurysm formation and progression in a novel model of thoracic aortic aneurysms. *Circulation*. 2014; 130: S51-59

36. Zhang D, Yan H, Hu Y, et al. Increased expression of NLRP3 inflammasome in wall of ruptured and unruptured human cerebral aneurysms: Preliminary results. *J Stroke Cerebrovasc Dis*. 2015; 24: 972-979

Figure Legends

Figure 1

Relationship between hemodynamic changes and the incidence of ruptured aneurysms at the anterior and posterior Willis circle

Representative vascular corrosion cast of a group 2 rat (A). Subarachnoid hemorrhage (SAH) after aneurysmal rupture was assessed stereomicroscopically in rats that died, exhibited abnormal behavior, or manifested a drastic loss in body weight in the course of 90 days. We inspected ruptured aneurysms at the anterior and posterior Willis circle (AW, PW) under a stereomicroscope after removing the blood coagulum (B). SAH-free survival was calculated based on the incidence of SAH (C) (**$p < 0.01$, log-rank test). On day 90 we prepared corrosion casts and calculated the total incidence of unruptured- and ruptured aneurysms at the AW and PW (D). **$p < 0.01$, †$p < 0.01$, Fisher's exact test.
ACA, anterior cerebral artery; BA, basilar artery; ICA, internal carotid artery; MCA, middle cerebral artery; OA, olfactory artery; P1, proximal portion of posterior cerebral artery

Figure 2

Relationship between hemodynamic changes and the incidence of unruptured aneurysms at the ACA-OA bifurcation

On day 90 we prepared corrosion casts. The right ACA-OA and the Willis circle on the casts were inspected at 2.5 kV under a scanning electron microscope. Representative aneurysms at the AW and PW were larger than aneurysms at the ACA-OA (A). There was no difference in the incidence of unruptured ACA-OA aneurysms between the two groups (B).

Figure 3

Representative elastica van Gieson (EvG) stain of ruptured PW aneurysms in group 2 rats

EvG stain of cross-sections of a ruptured PW aneurysm demonstrating a poorly organized luminal thrombus (T), disruption of the internal elastic lamina (DEL) in the intima, a decellularized (De), degenerated matrix (DM), and hyalinization (Hy) in the thickened media. The normal cerebral artery (CA) exhibits a continuous internal elastic lamina (EL) [(original magnification, x 40 (A), x 100 (B)].

Figure 4

Cerebral blood flow changes mirrored on ultrasonograms

Peak systolic velocity (PSV) (A) and end-diastolic velocity (EDV) (B) in the right ICA, the left ICA, and the BA were assessed ultrasonographically. The mean flow velocity (MFV) was calculated based on the PSV and the EDV (C). Representative ultrasonographic images mirrored the antegrade blood flow in the right ICA and the BA and the retrograde flow in the left ICA of experimental rats (D). *$p < 0.05$, **$p < 0.01$ by Tukey-Kramer test.

Figure 5

Relationship between the site and the incidence of ruptured aneurysms and the blood flow volume (BFVo)

We determined the vascular diameter (sham, n=13; group 1, n=24; group 2, n=13) on corrosion casts (A) after a 90-day observation period and calculated the BFVo in each artery. The BFVo of the BA was significantly greater in group 2 than group 1 rats (B). *$p < 0.05$, **$p < 0.01$, Tukey-Kramer test.

On day 90 the incidence of rupture of PW aneurysms was significantly higher in group 2- (n=26) than group 1 rats (n=27) (C). *$p < 0.05$, Fisher's exact test.

Figure 6

Gene expression of interleukin (IL)-1β and matrix degradation molecules

The mRNA level of IL-1β, matrix metalloproteinase (MMP)-9, and the tissue inhibitor of metalloproteinase (TIMP)2 in the vascular wall at the left P1 of sham-, group 1-, and group 2 rats (n=8 each group) was assessed by quantitative real-time polymerase chain reaction (qRT-PCR) assay (A). The expression of these molecules in the vascular wall at the right P1, ACA-OA, and left P1 in group 2 rats was also assessed by qRT-PCR (B). For normalization we used the mRNA level of glyceraldehyde 3-phosphate dehydrogenase (GAPDH).

*$p < 0.05$, **$p < 0.01$ by the Kruskal-Wallis test followed by the Mann-Whitney test or the Wilcoxon signed-rank test with Bonferroni correction.

ns; not significant

Figure 7

The effects of IL-1β on human brain vascular smooth muscle cells (HBVSMCs) *in vitro* and schematic illustration of our novel cerebral aneurysm model

HBVSMCs were exposed for 24 hr to IL-1β (1 ng/ml) and the mRNA level of MMP-9 and TIMP2 was determined by qRT-PCR assay (A). For normalization we used the mRNA level of GAPDH. After 24-hr treatment with IL-1β (1 ng/ml), cell proliferation was determined

with the Cell Counting Kit-8 (B). **p < 0.01 by the Mann-Whitney *U*-test. N.D., not detectable

Increased levels of pro-inflammatory cytokines and matrix degradation molecules induced by estrogen deficiency, hypertension, and hemodynamic stress resulted in the rupture of aneurysms at the AW and PW (C).

Figure 1

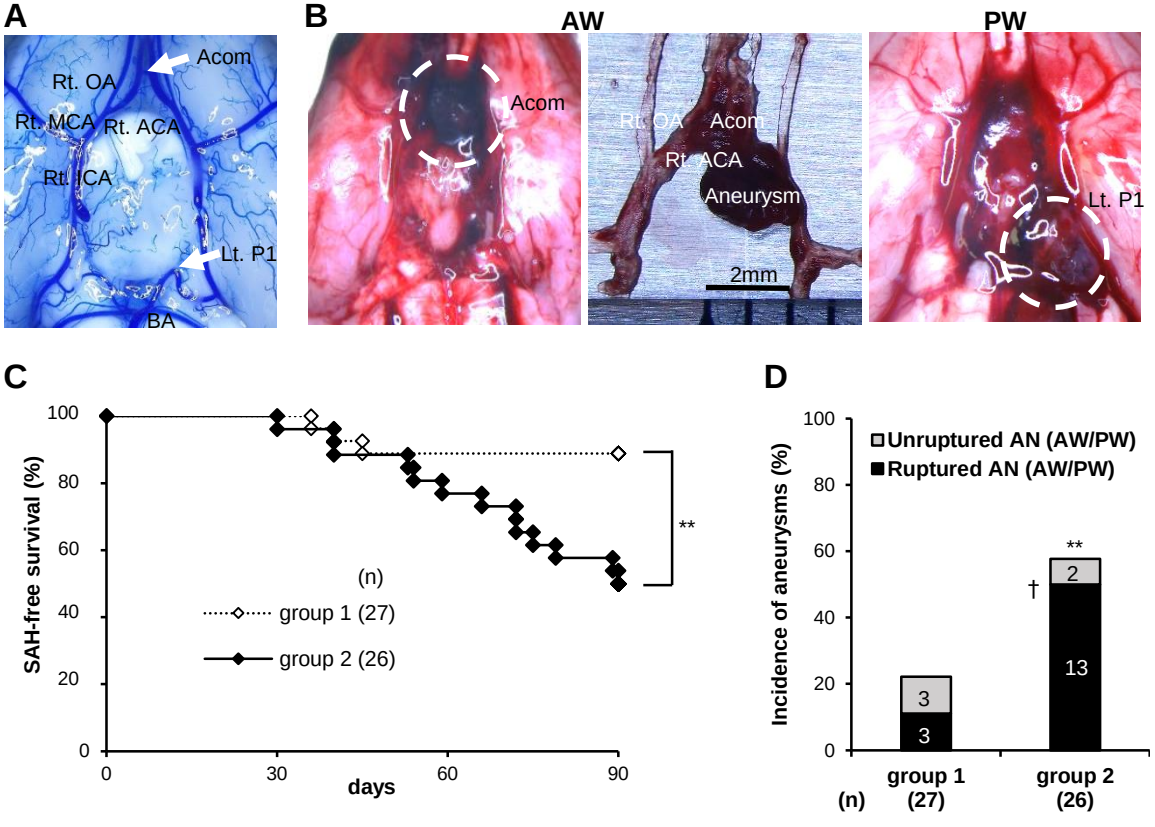
A
Acom
Rt. OA
Rt. MCA
Rt. ACA
Rt. ICA
Lt. P1
BA
B
AW
PW
Acom
Rt. OA
Acom
Rt. ACA
Aneurysm
2mm
Lt. P1
C
SAH-free survival (%)
100
80
60
40
20
0
0
30
60
90
days
(n)
group 1 (27)
group 2 (26)
**
D
Incidence of aneurysms (%)
Unruptured AN (AW/PW)
Ruptured AN (AW/PW)
**
†
2
13
3
3
group 1
(27)
group 2
(26)
(n)

Figure 2

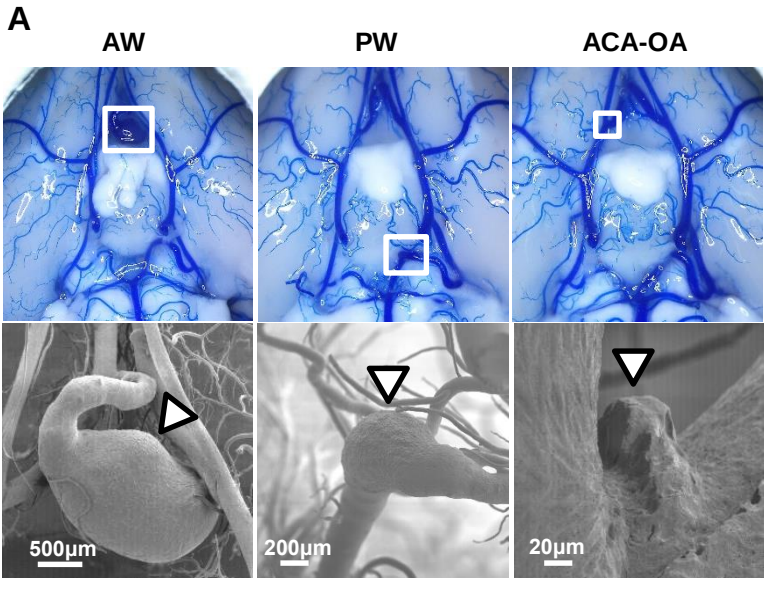
A
AW
PW
ACA-OA
500μm
200μm
20μm

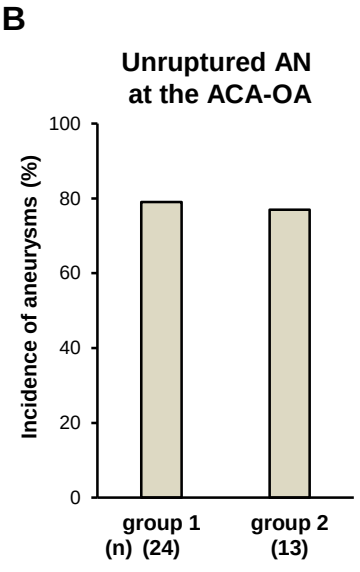
B
Unruptured AN
at the ACA-OA
Incidence of aneurysms (%)
100
80
60
40
20
0
group 1
(n) (24)
group 2
(13)

Figure 3

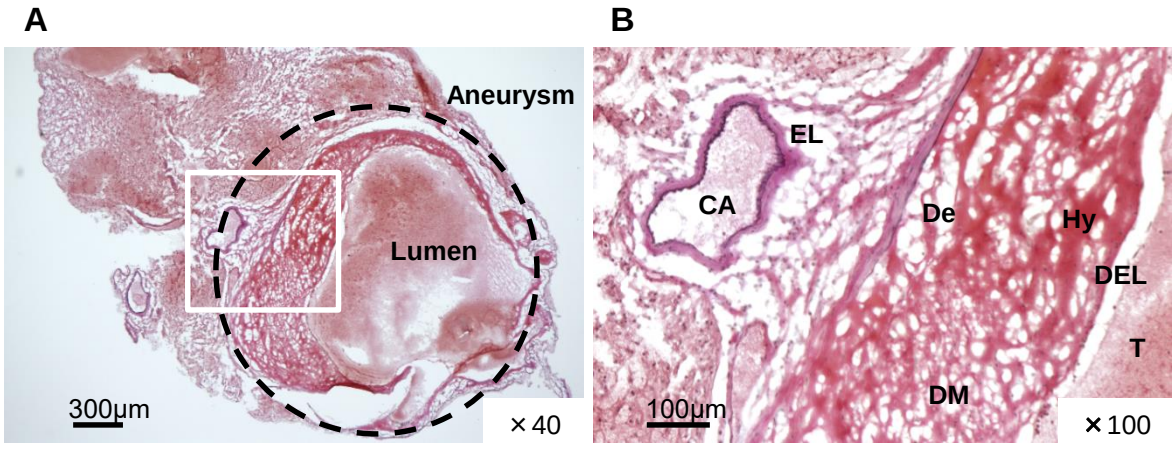

Figure 4

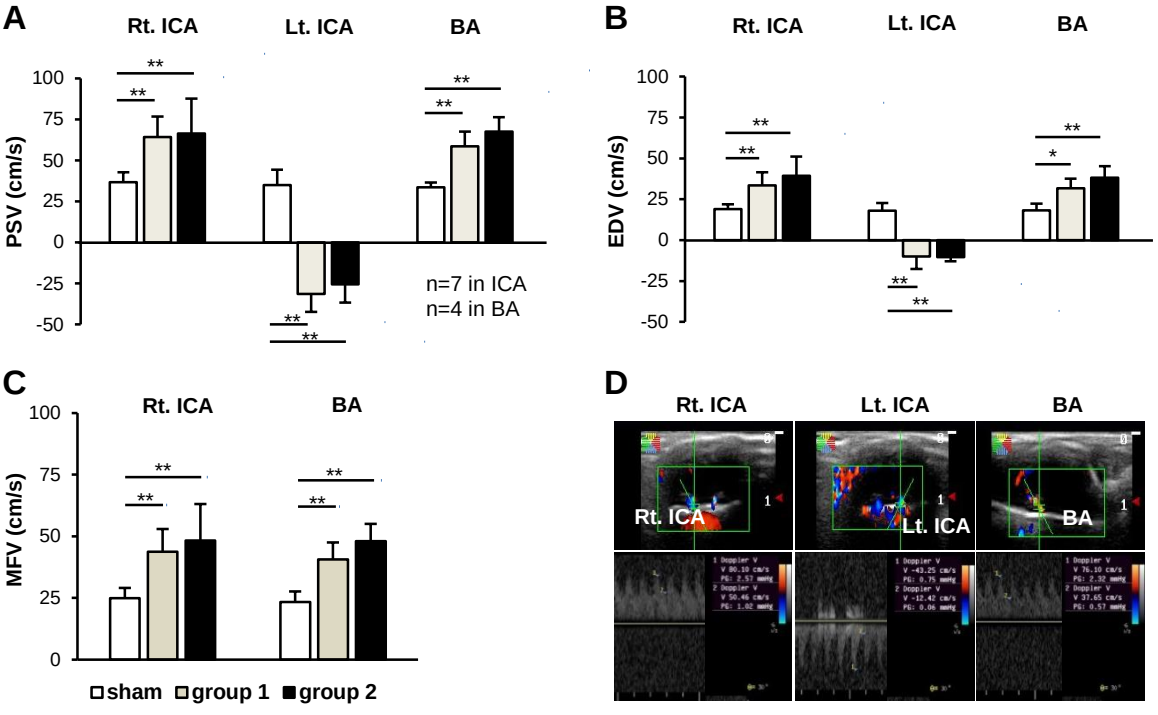
A
Rt. ICA
Lt. ICA
BA
PSV (cm/s)
100
75
50
25
0
-25
-50
**
n=7 in ICA
n=4 in BA
B
Rt. ICA
Lt. ICA
BA
EDV (cm/s)
100
75
50
25
0
-25
-50
**
*
C
Rt. ICA
BA
MFV (cm/s)
100
75
50
25
0
**
sham
group 1
group 2
D
Rt. ICA
Lt. ICA
BA

Figure 5

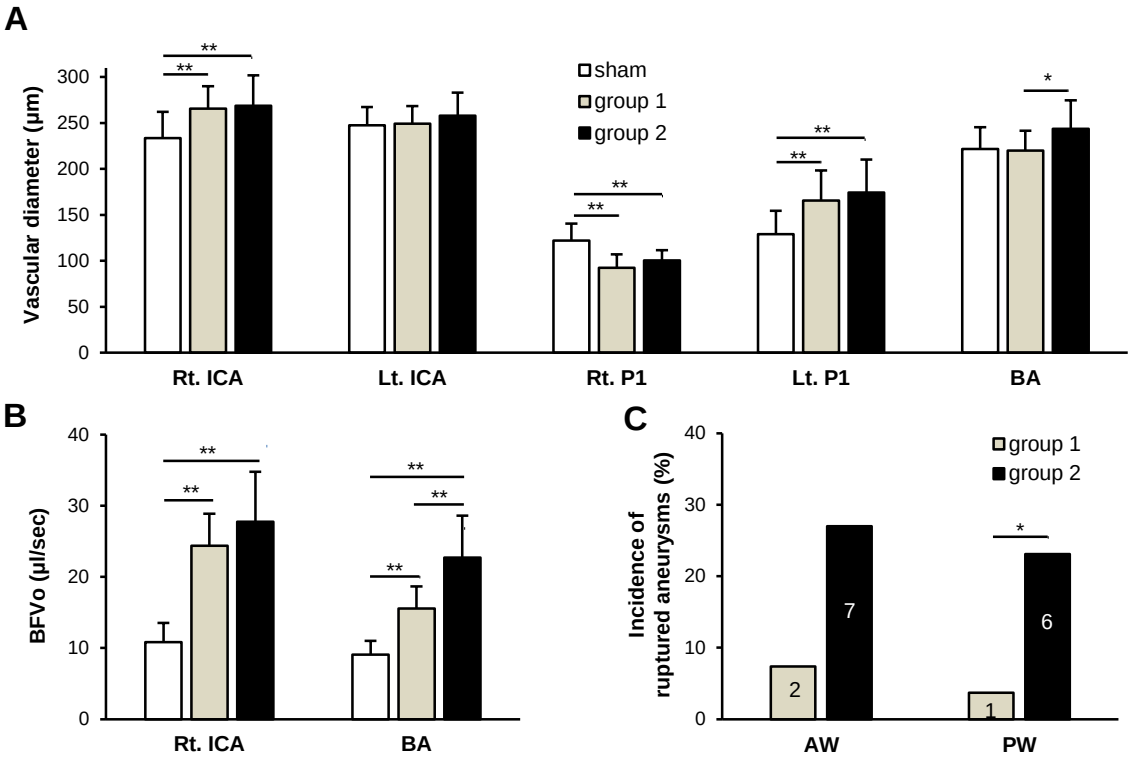
A
Vascular diameter (μm)
300
250
200
150
100
50
0
sham
group 1
group 2
**
**
**
**
**
**
*
Rt. ICA
Lt. ICA
Rt. P1
Lt. P1
BA
B
BFVo (μl/sec)
40
30
20
10
0
**
**
**
**
**
Rt. ICA
BA
C
Incidence of ruptured aneurysms (%)
40
30
20
10
0
group 1
group 2
*
2
7
1
6
AW
PW

Figure 6

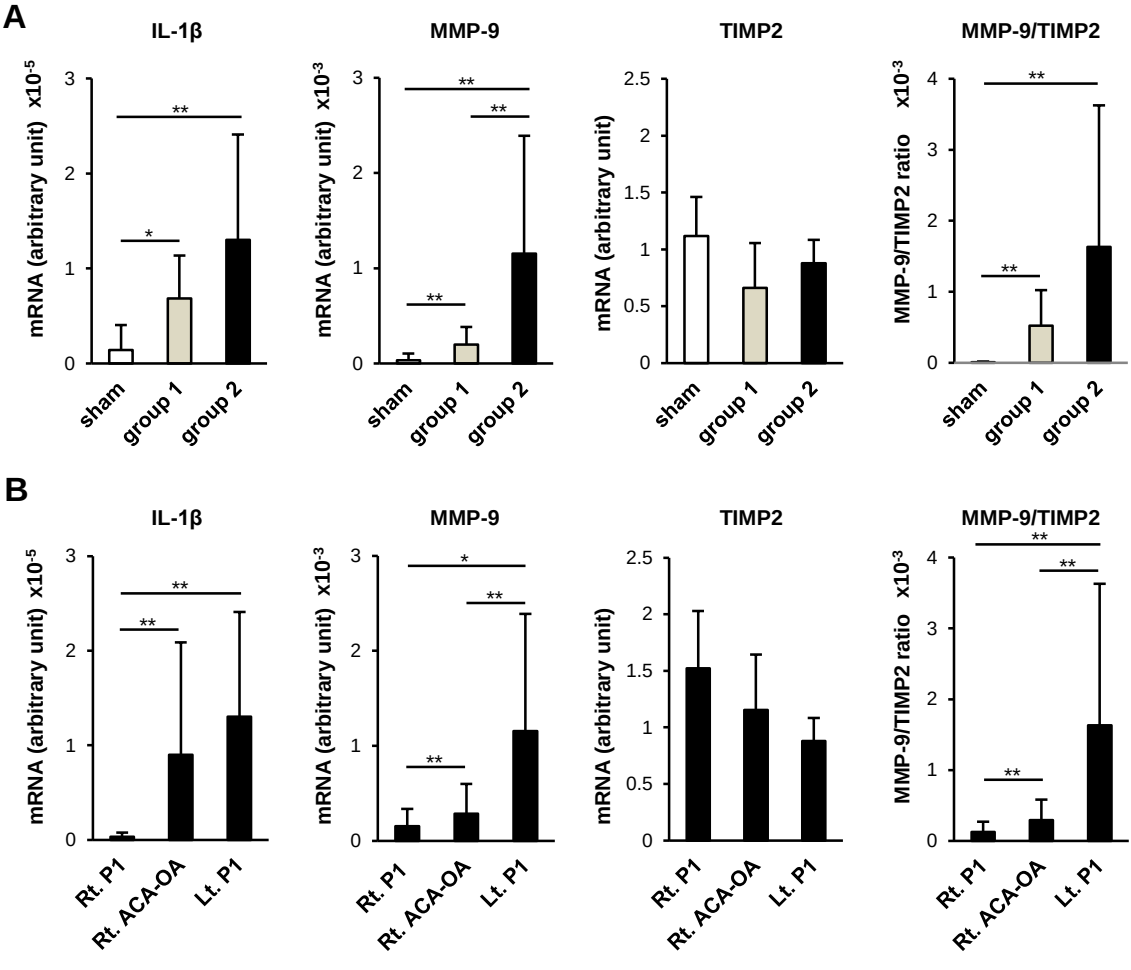
A
IL-1β
MMP-9
TIMP2
MMP-9/TIMP2
mRNA (arbitrary unit) x10-5
mRNA (arbitrary unit) x10-3
mRNA (arbitrary unit)
MMP-9/TIMP2 ratio x10-3
sham
group 1
group 2
B
Rt. P1
Rt. ACA-OA
Lt. P1

Figure 7

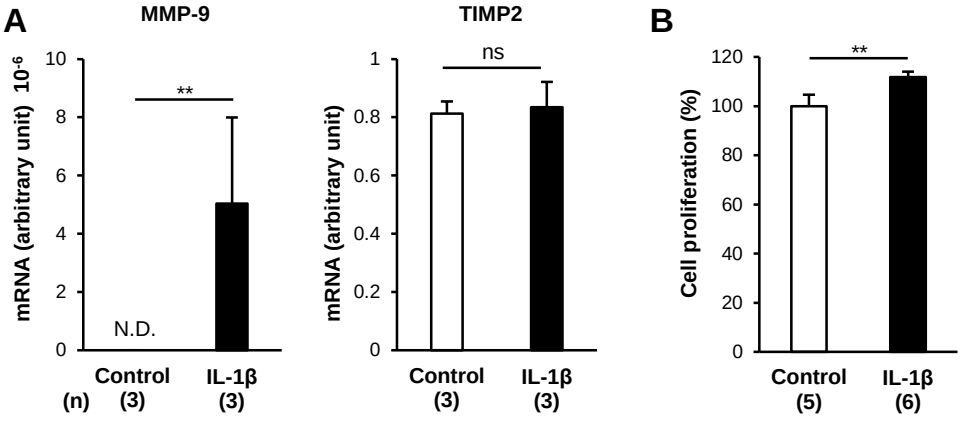
A
MMP-9
mRNA (arbitrary unit) 10-6
10
8
6
4
2
0
**
N.D.
Control
IL-1β
(n) (3) (3)
TIMP2
mRNA (arbitrary unit)
1
0.8
0.6
0.4
0.2
0
ns
Control
IL-1β
(3) (3)
B
Cell proliferation (%)
120
100
80
60
40
20
0
**
Control
IL-1β
(5) (6)

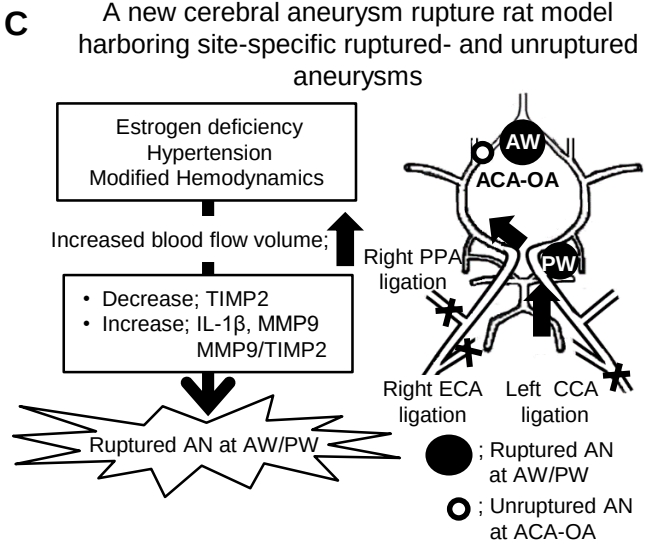
C
A new cerebral aneurysm rupture rat model harboring site-specific ruptured- and unruptured aneurysms
Estrogen deficiency
Hypertension
Modified Hemodynamics
Increased blood flow volume;
• Decrease; TIMP2
• Increase; IL-1β, MMP9
MMP9/TIMP2
Ruptured AN at AW/PW
AW
ACA-OA
PW
Right PPA ligation
Right ECA ligation
Left CCA ligation
; Ruptured AN at AW/PW
; Unruptured AN at ACA-OA

ONLINE SUPPLEMENT

Site-specific elevation of IL-1β and MMP-9 in the Willis circle by hemodynamic changes is associated with rupture in a novel rat cerebral aneurysm model

Takeshi Miyamoto[1] MD; David K. Kung[2] MD; Keiko T. Kitazato[1] BS;
Kenji Yagi[1] MD, PhD; Kenji Shimada[1] MD, PhD; Yoshiteru Tada[1] MD, PhD;
Masaaki Korai[1] MD; Yoshitaka Kurashiki[1] MD; Tomoya Kinouchi[1] MD, PhD;
Yasuhisa Kanematsu[1] MD, PhD; Junichiro Satomi[1] MD, PhD;
Tomoki Hashimoto[3] MD; Shinji Nagahiro[1] MD, PhD

[1]Department of Neurosurgery, Institute of Biomedical Sciences, Tokushima University Graduate School, Tokushima, Japan
[2]Department of Neurosurgery, University of Pennsylvania, Philadelphia, USA
[3]Department of Anesthesia and Perioperative Care, University of California, San Francisco, USA

Correspondence to:
Takeshi Miyamoto, MD
Department of Neurosurgery
Institute of Biomedical Sciences
Tokushima University Graduate School
3-18-15 Kuramoto-cho, Tokushima 770-8503, Japan

TEL: 81-88-633-7149
FAX: 81-88-632-9464
E-mail: takeshi_edit@yahoo.co.jp

Supplemental Materials and Methods

Blood pressure measurement

To record their blood pressure before and 30 and 90 days after bilateral posterior renal artery ligation (RAL) the rats were placed on a 37°C hot plate (NISSIN, Tokyo,

Japan) and covered with a black blanket. After acclimatization, one blinded examiner recorded their systolic- and diastolic- blood pressure based on 2 measurements obtained with the tail-cuff method (Softron, Tokyo, Japan).

Transcranial duplex ultrasonography

The rats were subjected to ultrasound imaging under isoflurane anesthesia using an ultrasonograph (S6V, Sonoscape, China) equipped with a 5-10 MHz linear transducer (10I2). They were placed on a heating plate (37ºC) to avoid anesthesia-induced hypothermia. Imaging was in the right lateral decubitus position. Briefly, the intracranial arteries were identified on color-coded Doppler images based on the arterial anatomy. The bilateral ICAs (n=7 per group) and the basilar artery (BA; n=4 per group) were examined 4 weeks after RAL by simple random sampling without replacement.

Coronal and medial sagittal cross-sectional views showed the intracranial ICAs and the BA, respectively. On cross-sectional views a pulsed sample was placed on the longitudinal axis of the right and left ICA; on medial sagittal cross-sectional views it was placed on the BA. Blood flow velocity (BFVe) waveforms were then recorded with optimal angle-correction between the Doppler beam and the long axis of the examined arteries. Ultrasound color-coded Doppler images and BFVe waveforms were transferred to an ultrasound image workstation for the subsequent analysis of the peak systolic and the end-diastolic blood flow velocity (PSV, EDV) and the mean flow velocity (MFV). The blood flow volume (BFVo)[1] was calculated as:

$$MFV\ (v) = (PSV\text{-}EDV)/3 + EDV$$

$$BFVo = 1/4\ \pi r^2 v\ (r = \text{the vessel diameter})$$

Preparation of vascular corrosion casts

Vascular corrosion casts were prepared as previously described.[2] The rats were transcardially perfused with heparinized phosphate-buffered saline (20 U/ml) and then Batson's No. 17 plastic (Polyscience Inc., Warrington, PA, USA). The right ACA-OA and the Willis circle on the casts were inspected at 2.5 kV under a scanning electron microscope. Three blinded examiners consensually graded the aneurysmal changes. To determine the vascular diameter, they manually outlined regions of interest (ROIs) on images of each artery using NIH ImageJ software. We compared experimental rats (group1; n=24, group 2, n=13) with age-matched sham-operated rats (n=13).

Histopathology

We inspected a ruptured PW aneurysm from a group 2 rat with drastic weight loss on day 40. The aneurysm was fixed with 99.5% ethanol for 24 hr, immersed in 10% sucrose for 24 hr, and then in 20% sucrose for another 24 hr. It was subsequently embedded in optimal cutting temperature compound (Tissue-Tek; Sakura, CA, USA), cut into 5-μm thin sections using a Leica CM1850 (Leica, Wetzlar, Germany), and mounted on silane-coated slides (Matsunami Glass, Tokyo, Japan). Elastica van Gieson stain was then applied to the specimens. An all-in-one microscope (BZ-X710, KEYENCE, Osaka, Japan) was used for observation.

RNA isolation and qRT-PCR assay

Samples from another set of sham-operated-, group 1- and group 2 rats (n=8 each) were subjected to qRT-PCR assay. Five weeks after RAL these rats were euthanized and total RNA from the right ACA-OA, the right P1 and the left P1 was isolated and extracted. At the time of sampling no aneurysms had ruptured. Total RNA was extracted with the EZ1 RNA Universal Tissue kit (QIAGEN, Tokyo, Japan) and placed in a MagNA lyser (Roche, Tokyo, Japan). For reverse transcription of total RNA to cDNA we used the transcriptor first-strand cDNA synthesis kit (Roche). qRT-PCR of each sample was in a LightCycler 2.0 (Roche). LightCycler FastStart DNA master and SYBR green I (Roche) were used for matrix metalloproteinase (MMP)-9, tissue inhibitor of metalloproteinase (TIMP)2, IL-1β, IL-6, tumor necrosis factor (TNF)-α, and glyceraldehyde 3-phosphate dehydrogenase (GAPDH). The primers for MMP-9 were forward primer (F), 5'-ACA ACG TCT TTC ACT ACC AA-3'; reverse primer (R), 5'-CAA AAG AGG AGC CTT AGT TC-3'; for TIMP2, F, 5'-CCC TCT GTG ACT TTA TTG TGC-3', R, 5'-TGA TGC TCT TCT CTG TGA CC-3'; for IL-1β, F, 5'-TGC AGG CTT CGA GAT GAA C-3', R, 5'-AGC TCA TGG AGA ATA CCA CTT G-3'; for IL-6, F, 5'-TCT CAG GGA GAT CTT GGA AAT G-3', R, 5'-TAG AAA CGG AAC TCC AGA AGA C-3'; for TNF-α, F, 5'-CCC AAC AAG GAG GAG AAG T-3', R, 5'-CGC TTG GTG GTT TGC TAC-3'; and for GAPDH they were F, 5'-TAC ACT GAG GAC CAG GTT G-3', R, 5'-CCC TGT TGC TGT AGC CAT A-3'.

After 24-hr treatment of HBVSMCs with IL-1β, total RNA was isolated and extracted with the MagNA Pure Compact kit (Roche). For reverse transcription of total RNA to cDNA we used Transcriptor Universal cDNA Master (Roche). qRT-PCR of each sample was in a LightCycler 2.0. LightCycler FastStart DNA master and SYBR green I were used for MMP-9, TIMP2, and GAPDH. The primers for MMP-9 were F, 5'-GGG ACG CAG ACA TCG TCA TC-3', R, 5'-TCG TCA TCG TCG AAA TGG GC-3'; for TIMP2, F, 5'-AAG CGG TCA GTG AGA AGG AAG-3',R, 5'-GGG GCC GTG TAG ATA

AAC TCT AT-3'; and for GAPDH, F, 5'-GGG TGT GAA CCA TGA GAA GTA TGA-3', R, 5'-TGC TAA GCA GTT GGT GGT GC-3'.

The results were quantified after normalization to the expression of GAPDH mRNA. The PCR conditions were 95ºC for 10 min followed by 45 cycles at 95ºC for 10 sec, 60ºC for 10 sec, and 72ºC for 8 sec. Cycle threshold values > 40 were considered to be below the detection level of the assay. We subjected samples from each group to two independent qRT-PCR assays.

Supplemental References

1. Kreis D, Schulz D, Stein M, Preuss M, Nestler U. Assessment of parameters influencing the blood flow velocities in cerebral arteries of the rat using ultrasonographic examination. *Neurol. Res*. 2011;33:389-395
2. Jamous MA, Nagahiro S, Kitazato KT, Satoh K, Satomi J. Vascular corrosion casts mirroring early morphological changes that lead to the formation of saccular cerebral aneurysm: An experimental study in rats. *J. Neurosurg*. 2005;102:532-535

Supplemental Figure I

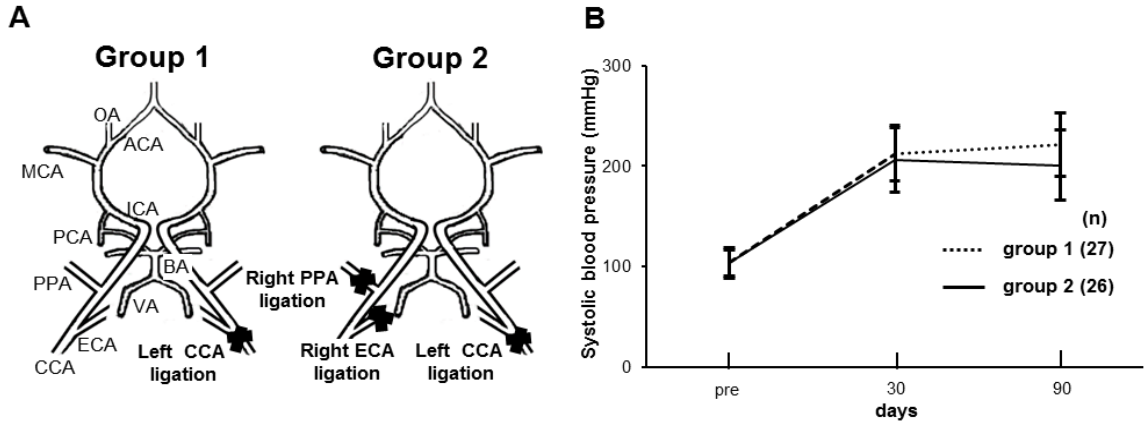

Ligation of carotid arteries and blood pressure changes

To induce hemodynamic changes the rats were divided into 2 groups (A). Group 1 was subjected to ligation of the left common carotid artery (CCA). Group 2 underwent additive ligation of the right pterygopalatine artery (PPA) and the right external carotid artery (ECA). There was no difference in the blood pressure of the 2 groups by Student's *t* test (B).

ACA, anterior cerebral artery; BA, basilar artery; ECA, external carotid artery; ICA, internal carotid artery; MCA, middle cerebral artery; OA, olfactory artery; PCA, posterior cerebral artery; VA, vertebral artery.